

In the format provided by the authors and unedited.

Physical activation of innate immunity by spiky particles

Ji Wang^{1,2,3}, Hui-Jiuan Chen^{1,3}, Tian Hang¹, Yang Yu², Guishi Liu^{1,2}, Gen He¹, Shuai Xiao¹, Bo-ru Yang¹, Chengduan Yang¹, Fanmao Liu¹, Jun Tao¹, Mei X. Wu^{2*} and Xi Xie^{1*} 

¹State Key Laboratory of Optoelectronic Materials and Technologies, School of Electronics and Information Technology, Guangdong Province Key Laboratory of Display Material and Technology, The First Affiliated Hospital of Sun Yat-Sen University, Sun Yat-Sen University, Guangzhou, China.

²Wellman Center for Photomedicine, Massachusetts General Hospital, Department of Dermatology, Harvard Medical School, Boston, MA, USA. ³These authors contributed equally: Ji Wang, Hui-Jiuan Chen. *e-mail: mwu5@mgh.harvard.edu; xiexi27@mail.sysu.edu.cn

S1. The spiky morphology of representative microbes.

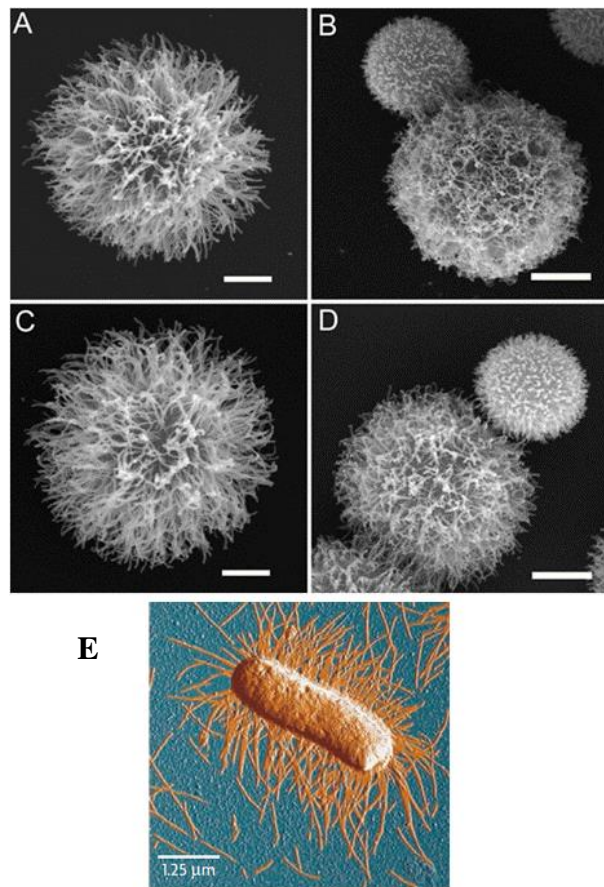
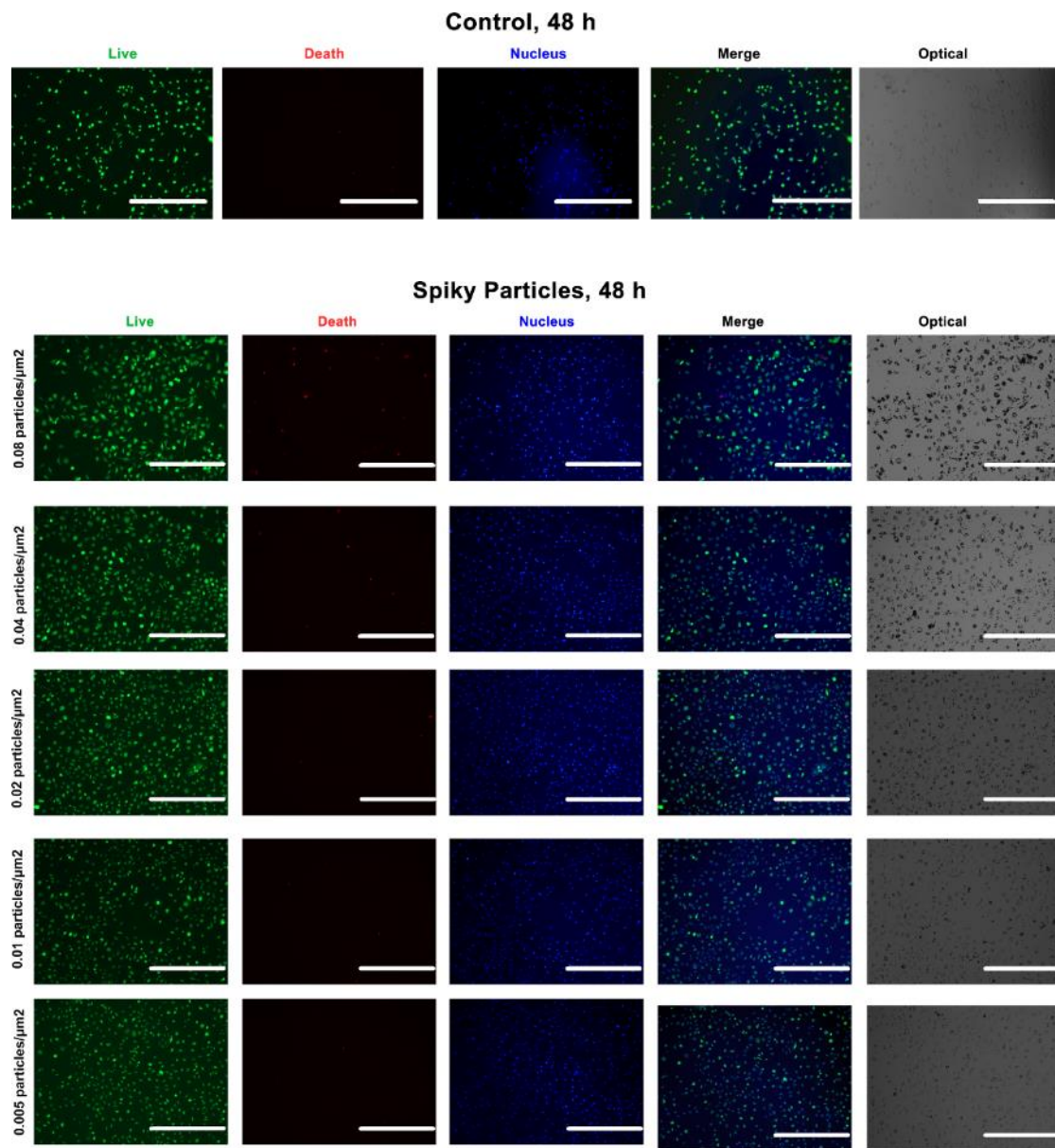


Figure S1. SEM images of *C. neoformans* yeast cells (A-D) with reprint permission from Ref. [1]. Scale bars: 2 μm . A SEM image of *E. Coli* (E) is reprinted with permission from Ref. [2].

S2. Supplemental information for macrophage viability upon particle treatments.



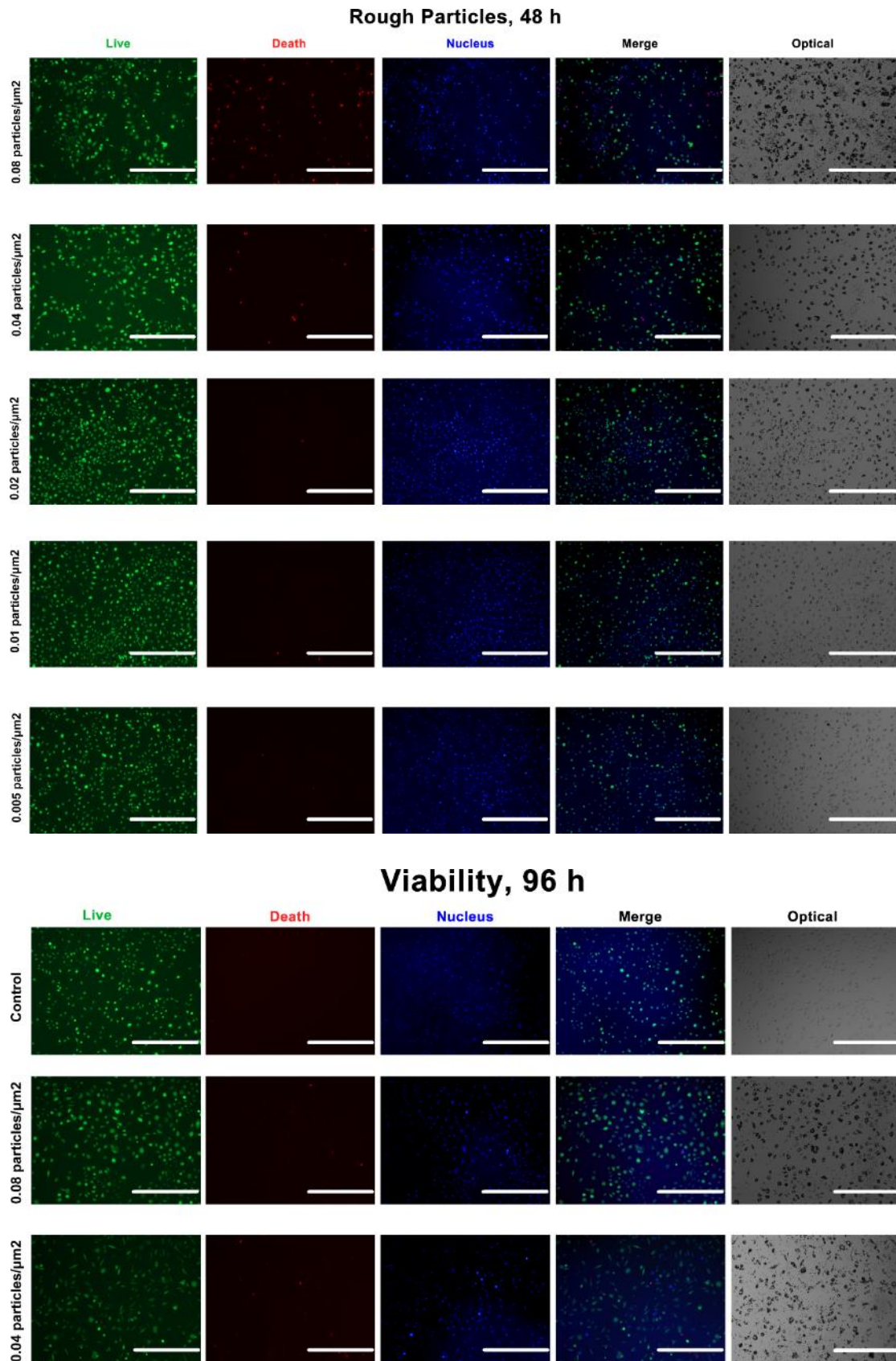


Figure S2. Fluorescence and optical images of BMMs after incubation with spiky particles or rough particles at different particle doses. Green, live cells; Red, dead cells; and Blue, cell nucleus. Scale bar: 400 μm . All experiments were repeated twice with

similar results.

S3. Spiky particles did not significantly affect the metabolic activities.

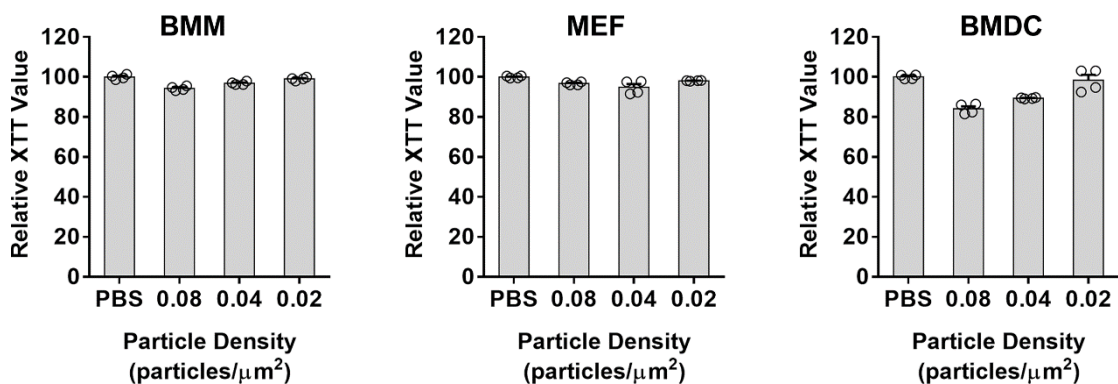


Figure S3. Spiky particles did not significantly affect the metabolic activities. Mouse primary cells, including BMMs, MEFs and BMDCs were cultured with Spiky particles at 0.02-0.08 particles/μm² for 72 hours. The metabolic activities were measured by a XTT assay and normalized to PBS controls. n=4 biologically independent samples. All experiments were repeated twice with similar results. Data were presented as Mean±SEM.

S4. Spiky particles did not induce apoptosis.

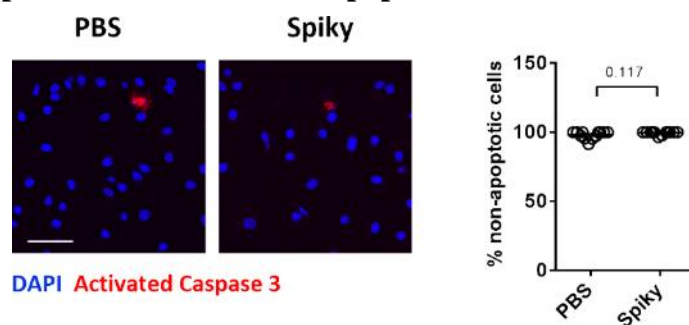


Figure S4. Spiky particles did not induce apoptosis. BMMs were cultured with Spiky particles at a dose of 0.08 particles/μm² for 72 hours. Cells were fixed, stained for active Caspase-3 and imaged by confocal microscopy. Scale bar: 50 μm. Percentages of non-apoptotic cells in 12 fields were summarized on the right. Data were presented as Mean±SEM. n= 12 biologically independent samples. The experiment was repeated twice with similar results. Significance was calculated by two-tailed t-test.

S5. Supplemental information for cell-particle interface.

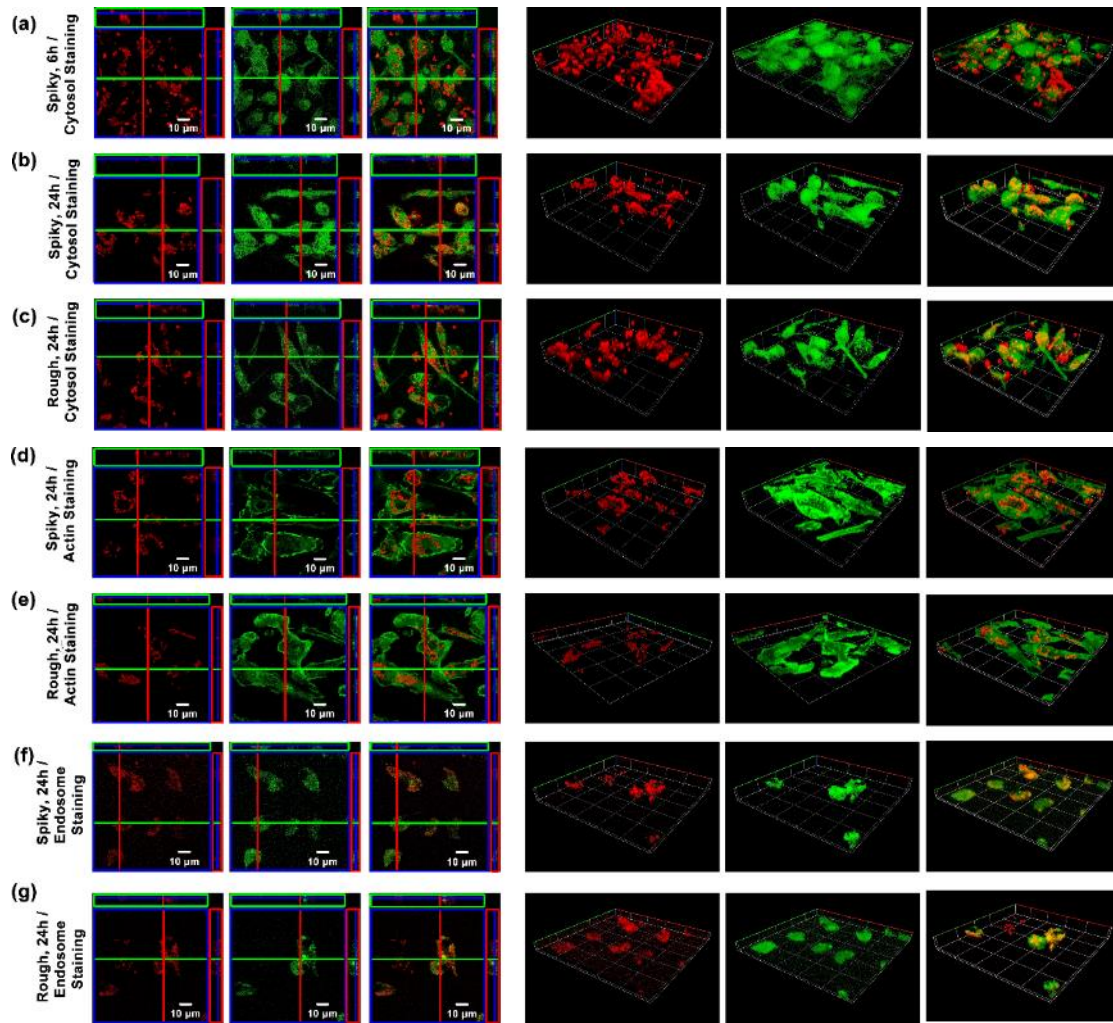


Figure S5. BMM-particle interface study via confocal fluorescence microscopy. (a)-(c) BMMs (cytosol labeled with green fluorescence) interfaced with spiky particles or rough particles for 24 h, or with spiky particles for 6 h. Green, cell cytosol and Red, particles. (d) and (e) The interface between BMMs' actin networks and spiky particles or rough particles in 24 h of particle incubation. (f) and (g) Green, cell actin network and Red, particles. Spiky particles or rough particles entrapped in cell endosomes after 24 h of particle incubation. Green, cell endosomes and Red, particles. All experiments were repeated twice with similar results.

S6. Endotoxin test for particles.

The endotoxin levels of the fabricated spiky particles, rough particles, and nanorods were analyzed. The particles and nanorods in endotoxin-free water were sonicated for 12 h and centrifuged at 18,000 rcf for 8 min. The upper solution was collected for analysis of endotoxin levels using the Thermo Scientific™ Pierce™ LAL Chromogenic Endotoxin Quantitation Kit (Thermo Scientific).

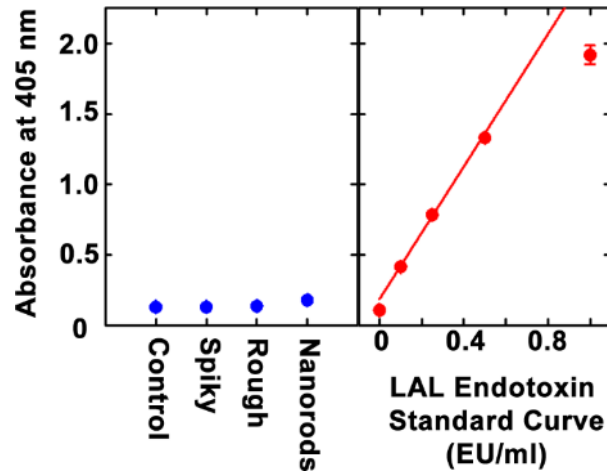
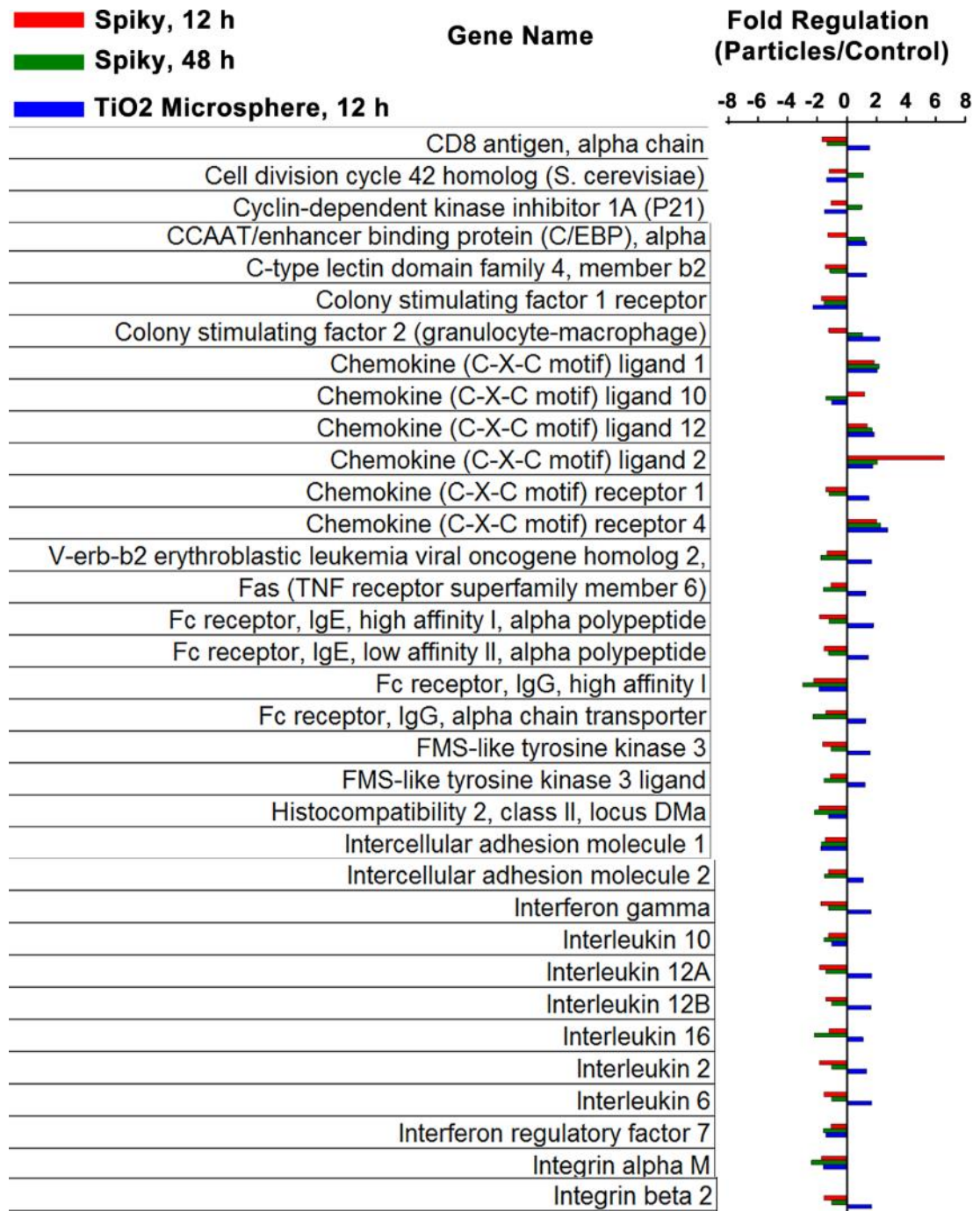
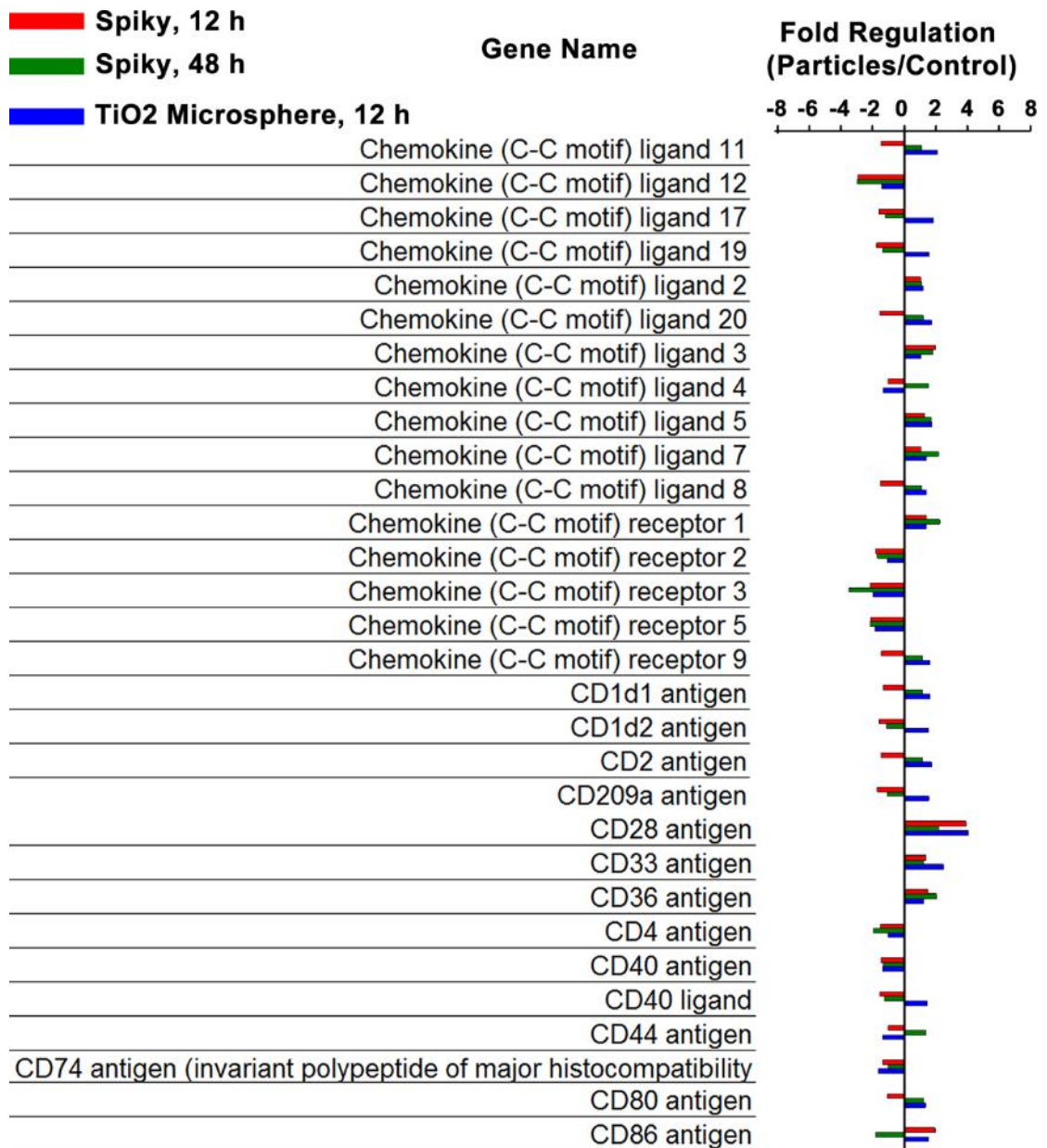


Figure S6. The limulus Amebocyte Lysate (LAL) endotoxin standard curve was plotted as red color, and the solution from spiky particles, rough particles, nanorods and control group (endotoxin-free water) were plotted as blue color. The endotoxin level of the spiky particles, rough particles and nanorods were not significantly higher compared to the endotoxin-free water control. The experiment was repeated three times with similar results. Data were presented as Mean \pm SEM.

S7. Supplemental information for gene profiling.





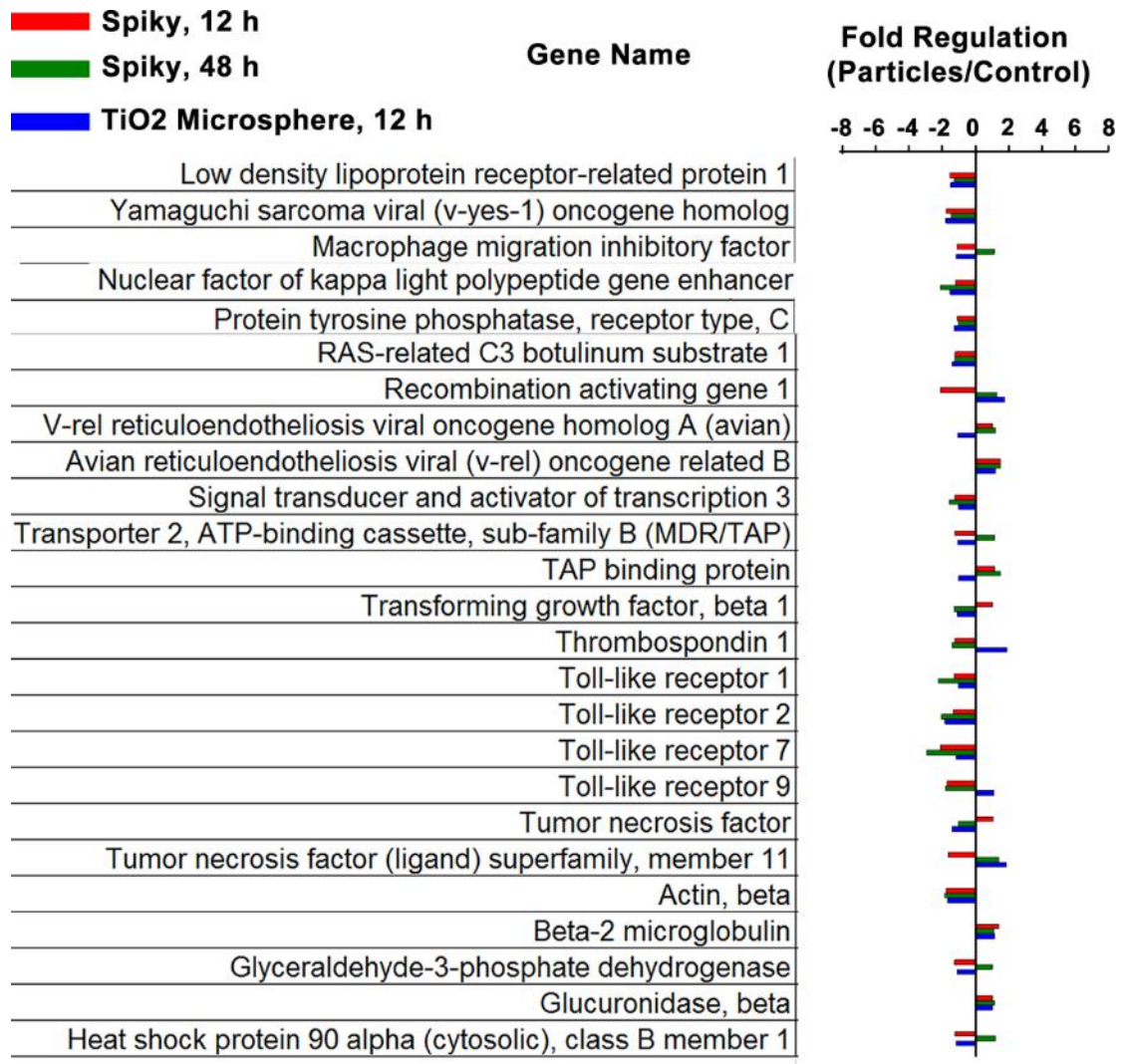


Figure S7. The expression profiles of 89 genes that are important for cell inflammatory activation such as cytokines, chemokines and their corresponding receptors, as well as antigen uptake, processing and presentation. The gene profiles were analyzed by quantitative real-time RT-PCR. The expression levels were compared with the control groups without particle treatments. The results were re-plotted as Figure 4a in the main text, with solid line indicating no change between control and treated cells, while two dash lines indicated 2 fold up- or down-regulation, respectively.

S8. Spiky particles did not promote M1 or M2 polarization of macrophages.

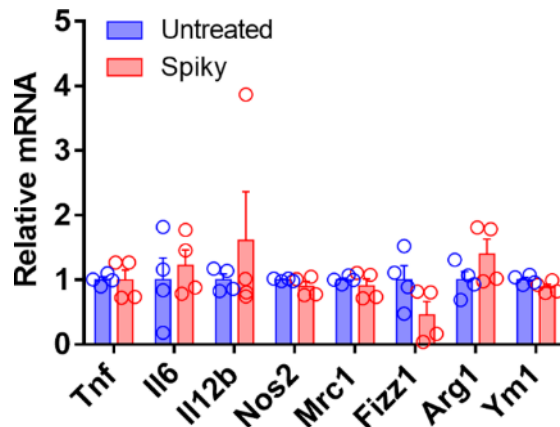


Figure S8. Spiky particles did not promote M1 or M2 polarization of macrophages. BMMs were cultured with Spiky particles at a dose of 0.04 particles/ μm^2 for 12 hours. The mRNA level of M1 markers (Tnf, Il6, Il12b and Nos2) and M2 markers (Mrc1, Fizz1, Arg1 and Ym1) were analyzed by real-time RT-PCR. mRNA levels were first normalized to Gapdh and then normalized to untreated controls. n=4 biologically independent samples. The experiment was repeated twice with similar results. Data were presented as Mean \pm SEM.

Table S1. Primers for real-time RT-PCR analysis of M1 and M2 macrophage subtypes

Gene name	Forward primer (5'-3')	Reverse primer (5'-3')
<i>Gapdh</i>	ATCAAGAAGGTGGTGAAGCA	AGACAACCTGGTCCTCAGTGT
<i>Tnf</i>	CCTGTAGCCCACGTCGTAG	GGGAGTAGACAAGGTACAACCC
<i>Il6</i>	TAGTCCTTCTACCCCAATTTC	TTGGTCCTTAGCCACTCCTTC
<i>Il12b</i>	TGTGGAATGGCGTCTCTGTC	AGTTCAATGGGCAGGGTCTC
<i>Nos2</i>	GGTGAAGGGACTGAGCTGTTA	TGAAGAGAACTTCCAGGGGC
<i>Mrc1</i>	GTGGAGTGATGGAACCCAG	CTGTCCGCCAGTATCCATC
<i>Fizz1</i>	GACTGCTACTGGGTGTGCTT	GCTGGGTTCTCCACCTCTTC
<i>Ym1</i>	CCAGTTGGGCTAAGGACAGG	CAGGTGAGTACACAGGCAGG
<i>Arg1</i>	GTGGGAATGGAGGACATGGG	GGATTAGCACCTGGTCCCG

S9. Impact of spiky particles on BMM viability in the presence of LPS or MPL.

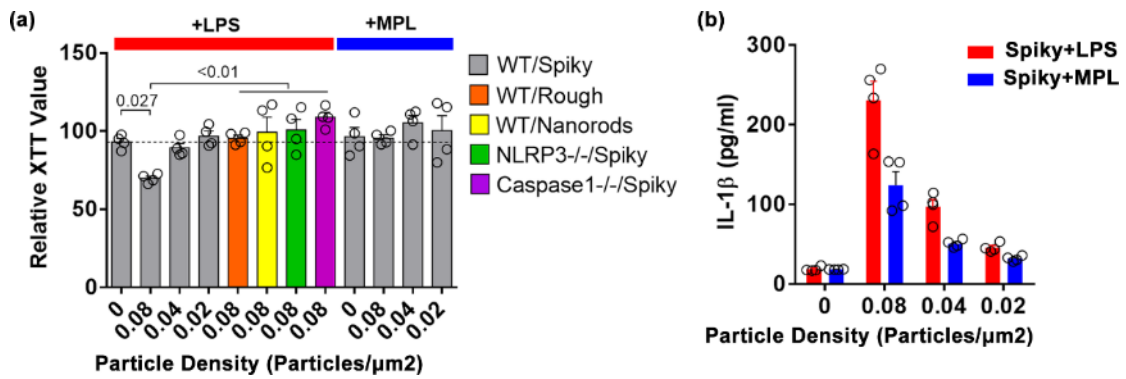


Figure S9. Cell viabilities after culturing with spiky particles in the presence of LPS or MPL. BMMs from WT, Caspase 1^{-/-} or NLRP3^{-/-} mice were stimulated with LPS or MPL for 3 h and then cultured with spiky particles, rough particles or nanorods at 0.02-0.08 particles/μm² for another 18 h. (a) The metabolic activities were measured via a XTT assay and normalized to the results of using LPS alone. n=4 biologically independent samples. (b) Release of IL-1β was measured by ELISA. n=4 biologically independent samples. All experiments were repeated twice with similar results. Data were presented as Mean±SEM. Significance between indicated groups was calculated by one-way ANOVA.

S10. Supplemental information illustrates the mechanism underlying inflammasome activation by spiky particles.

PAMPs comprise a variety of biochemical cues or microbial materials sensed by corresponding receptors in the host. For example, lipopolysaccharide (LPS) derived from bacterial cell wall is recognized by Toll-like receptor (TLR) 2 and 4, while bacterial CpG DNA and viral RNA are potent stimulators for TLR9 and TLR3, respectively.[3] Besides receptors located on the cell surface or endosomes, cytoplasmic receptors such as NOD-like receptors (NLR) are also capable of sensing microbial components like bacterial toxins, DNA, and Flagellin in the cytoplasm.[4] Once stimulated, some NLRs induce the formation of inflammasome, a protein complex that triggers a release of pro-inflammatory cytokines such as IL-1 β and the inflammasome is critically involved in adaptive immune responses.[5,6]

The possible mechanism for inflammasome activation by spiky particles is illustrated in Figure 4e in the main text and explained in more detail here.

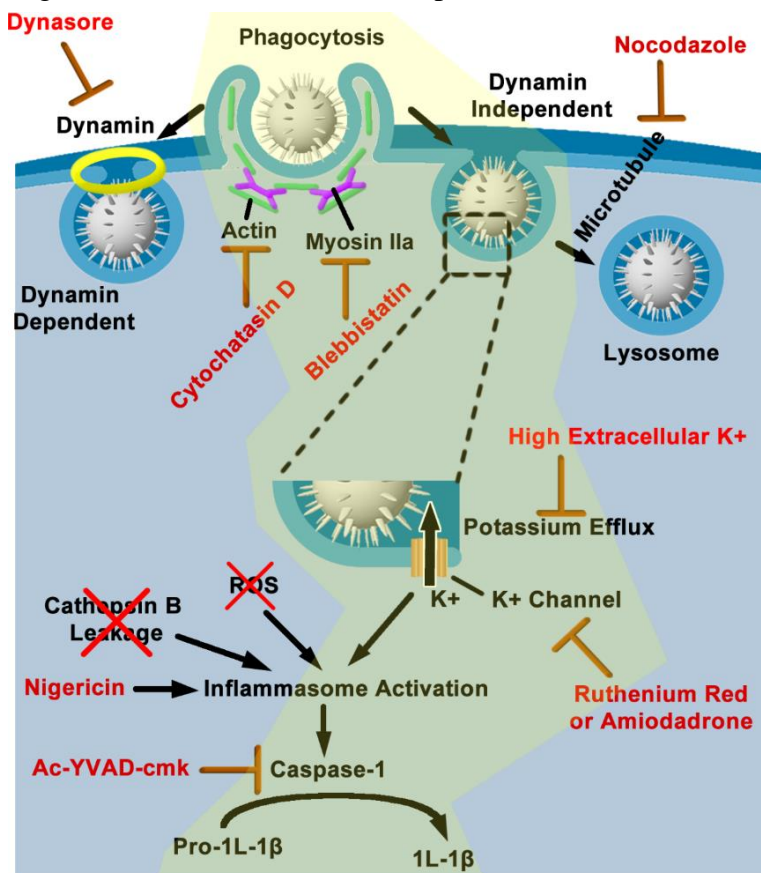


Figure S10. Illustration of inflammasome activation by spiky particles. The yellow region indicates the feasible mechanism revealed by experiments.

A particle is being engulfed by phagocytosis, a process that is mediated by actin filaments, in which myosin IIa is recruited to facilitate assembly of the actin filaments generating a mechanical force to phagocytize the particle. A phagocytosis inhibitor cytochalasin D specific for actin and blebbistatin specific for myosin IIa, either one can sufficiently abrogate the inflammasome activation evoked by spiky particles and thus, particle engulfment with a sufficient mechanical force is pivotal. On the contrary, dynasore failed to inhibit spiky particle-mediated activation of inflammasome. Dynasore blocks dynamins that is involved in forming a collar around the neck of the invagination and the scission of newly formed vesicles to form phagosomes after the invagination pinched off into a vesicle. The results suggested that the inflammasome activation is not dependent on dynamins and the vesicle pinching off is unlikely to be involved in the described inflammasome activation.

Although microtubules are important for the intracellular transport of phagosomes and subsequent fusion of phagosomes with lysosomes and have been known to promote the activation of inflammasome by driving spatial arrangement of mitochondria, microtubule-disrupting drug nocodazole failed to impede spiky particle-induced inflammasome activation, suggesting that both transformation of phagosomes and mitochondria arrangement are dispensable in the activation of inflammasomes. Some mineral crystals such as silica crystals are able to induce inflammasome activation via frustrated phagocytosis and release of cathepsin B into cytosol owing to damaged endosome membrane. However, spiky particles did not induce the release of cathepsin B into cytosol, in contrast to silica crystals that induced significant cathepsin B production in the cytosol, ruling out any role for frustrated phagocytosis in inflammasome activation via spiky particles. We also exclude a role for ROS in the activation despite the fact that ROS is a common activation factor of inflammasome, because incubation of BMMs with spiky particles did not increase intracellular ROS.

Accordingly, the inflammasome activation by spiky particles is mostly likely to occur during the first step when spiky particles are being engulfed prior to full internalization. In this regard, efflux of K^+ is a common mechanism associated with inflammasome activation. Indeed, when K^+ efflux is blocked by increasing extracellular K^+ concentration or an

inhibitor, amiodarone and to a lesser extent, ruthenium red, inflammasome activation is hindered by all three means either completely or at varying degrees, arguing strongly that K⁺ efflux is crucial for inflammasome activation evoked by spiky particles. As a few of mechanic tension-sensitive K⁺ channels are located on the cell membrane, we speculate that the nanospikes on particles may exert cellular force and mechanic stress on cell membrane during phagocytosis which in turn facilitates the activation of K⁺ channels.

S11. Mechanism underlying inflammasome activation by spiky particles.

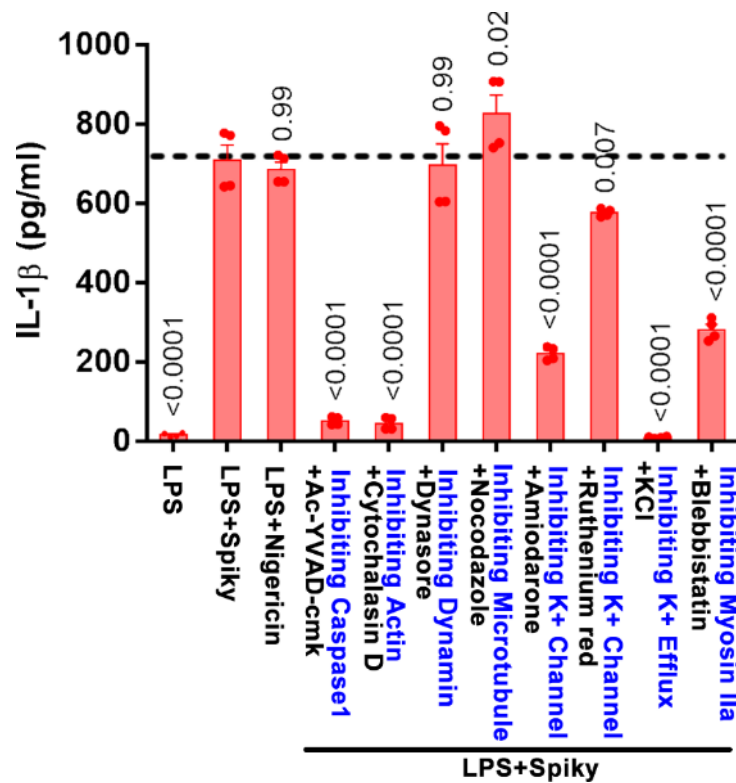


Figure S11. Exploration of the mechanism underlying inflammasome activation by spiky particles. Functions of specific inhibitors are indicated with blue text. BMMs were pretreated with indicated inhibitors for 0.5 h and treated with LPS and spiky particles. The dotted line indicates the mean of LPS+Spiky group. n=4 biologically independent samples. The experiment was repeated twice with similar results. Significance was calculated by one-way ANOVA, compared to LPS+Spiky.

S12. Theoretical Prediction of the Spiky Particles-mediated Stress on Cell Membrane.

Immune cell activation is presumably induced by the nanospikes-mediated extra stress on the cell membrane. As illustrated in Figure S12, the cell membrane coupled with the actin network underneath engulfs a particle through phagocytosis. In this process, the cell membrane along with actin network invaginates and forms a pocket around a particle, exerting forces on the particle by ATP-dependent molecular motors such as myosins. The particle in turn presses local stress on the cell membrane at a site of cell-particle contact. The cell sensed the local stress and responds by activation of some cellular pathways should the stress reach to certain thresholds.

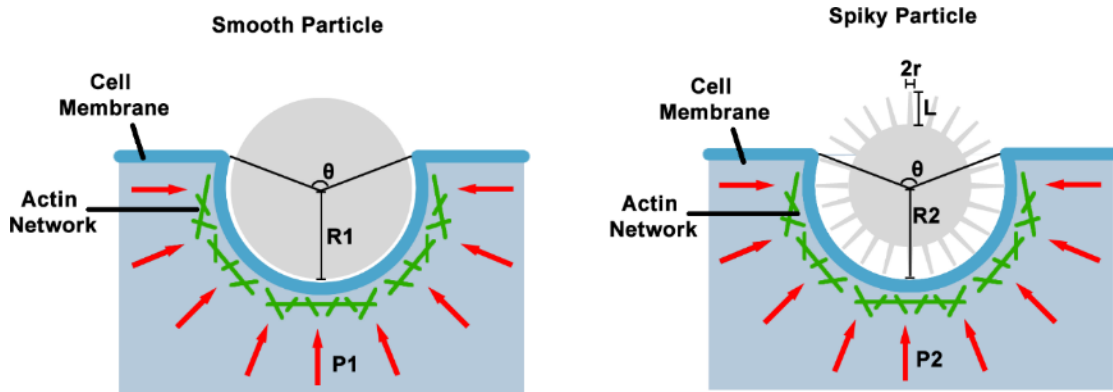


Figure S12. Depict of particles-mediated stress on cell membrane and parameters used in the theoretical calculation model.

The scenario of this process was shown in Figure S12. For a conventional spherical particle with smooth surface, the radius was defined as R_1 . The cell membrane along with actin network invaginates and forms a pocket with radius R_1 around the particle assuming the cell membrane conformally contacted with the particle. The cell membrane partially wrapped around the particle. The degree of surface contact can be defined by the angle θ as shown in the figure. Therefore, the surface area of the particle portion contacting with cell membrane was:

$$S_1 = 2\pi R_1^2 \cdot \left(1 + \cos \frac{\theta}{2}\right) \quad \text{Eq.(1)}$$

In order to compare spiky particle with smooth particle with the same size, the total radius of a spiky particle R_2 equals to R_1 . The length of the nanospike is L , the radius of a nanospike tip is r , and the total number of the nanospikes on a spiky particle surface was N . The surface area of the spiky particle portion contacting with cell membrane was:

$$S_2 = b \cdot \frac{N}{2} \pi r^2 \cdot (1 + \cos \frac{\theta}{2}) \quad \text{Eq.(2)}$$

Here b is coefficient to describe the state of the nanospikes contacting with cell membrane: $b=1$, if the nanospike perfectly contacts with the cell membrane as shown in the figure; $b<1$, should the nanospike is not fully covered by cell membrane; $b>1$, if the nanospike is over-covered by the cell membrane.

For the smooth particle, assuming the cellular force uniformly distributed on the cell membrane contacting with the particle, the total cellular force F_1 can be defined by:

$$F_1 = 2\pi R_1^2 \cdot (1 + \cos \frac{\theta}{2}) \cdot P_1 \quad \text{Eq.(3)}$$

Here P_1 is the uniform stress on the cell membrane for the smooth particle case.

For the spiky particle, assuming the cellular force uniformly distributed on the cell membrane contacting with the nanospikes, the total cellular force F_2 can be defined by:

$$F_2 = b \cdot \frac{N}{2} \pi r^2 \cdot (1 + \cos \frac{\theta}{2}) \cdot P_2 \quad \text{Eq.(4)}$$

Here P_2 is the uniform stress on the cell membrane for the spiky particle case.

The relation between P_1 and P_2 can be described by:

$$P_2 = \frac{F_2}{F_1} \cdot \frac{4R_1^2 \cdot P_1}{b \cdot N \cdot r^2} \quad \text{Eq.(5)}$$

For comparison, the total cellular forces was assumed to be the same for smooth particle and spiky particle ($F_1 = F_2$). From experimental results, the radius of a spiky particle $R_2 = R_1 = 900$ nm. The radius of a nanospike tip $r = 10$ nm. The total number of nanospikes on a particle N was estimated to be 645/particle. The nanospike-particle contact coefficient was 1 assuming perfect contact as shown in Figure S12. With all these given conditions, the relation between P_1 and P_2 was estimated to be:

$$P_2 \approx 50 \cdot P_1 \quad \text{Eq.(6)}$$

Based on this calculation result, the local stress on cell membrane for spiky particle can be 50 times higher than a smooth particle. On the other hand, based on the experimental results in main text Figure 4k, significant recruitment of myosin IIa was found around the phagocytized spiky particles, whereas such recruitment was negligible during the phagocytosis of rough particles. Inhibition of Myosin IIa by its specific inhibitor blebbistatin significantly blocked inflammasome activation provoked by spiky particles (main text Figure 4f). This result indicates that spiky particles mediated generation of stronger mechanical forces during phagocytosis: i.e. $F_2 > F_1$. From experimental results, the radius of a spiky particle $R_2 = R_1 = 900$ nm. The radius of a nanospike tip $r = 10$ nm. The total number of nanospikes on a particle N was estimated to be 645/particle. The nanospike-particle contact coefficient b was 1 assuming perfect contact as shown in Figure S12. With all these given conditions, the relation between P_1 and P_2 was estimated to be:

$$P_2 > 50 \cdot P_1 \quad \text{Eq.(7)}$$

Therefore, the local stress of a spiky particle on cell membrane is at least 50 times higher than that of a smooth particle.

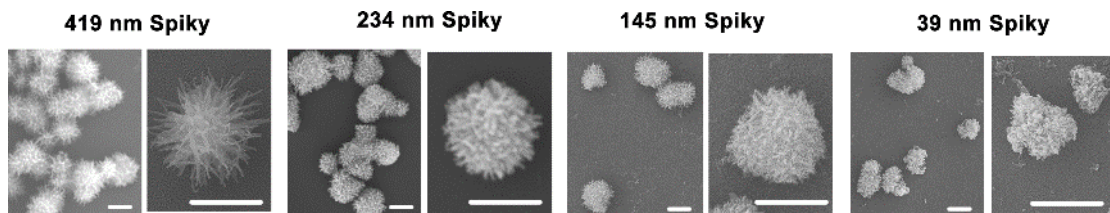


Figure S13. SEM images of particles with different spike lengths. Spiky particles with different nanospike lengths (419 ± 83 , 234 ± 56 , 145 ± 42 and 39 ± 17 nm) were fabricated by using sonication to selectively shorten the nanospikes. Scale bar, 1 μm . The experiment was repeated twice with similar results.

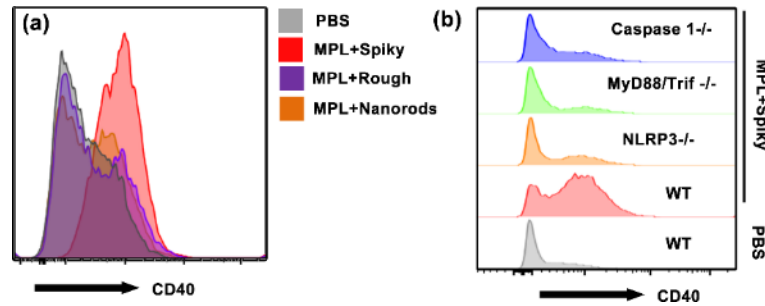


Figure S14. Representative flow cytometry data for Fig. 5b (a) or Fig. 5c (b).

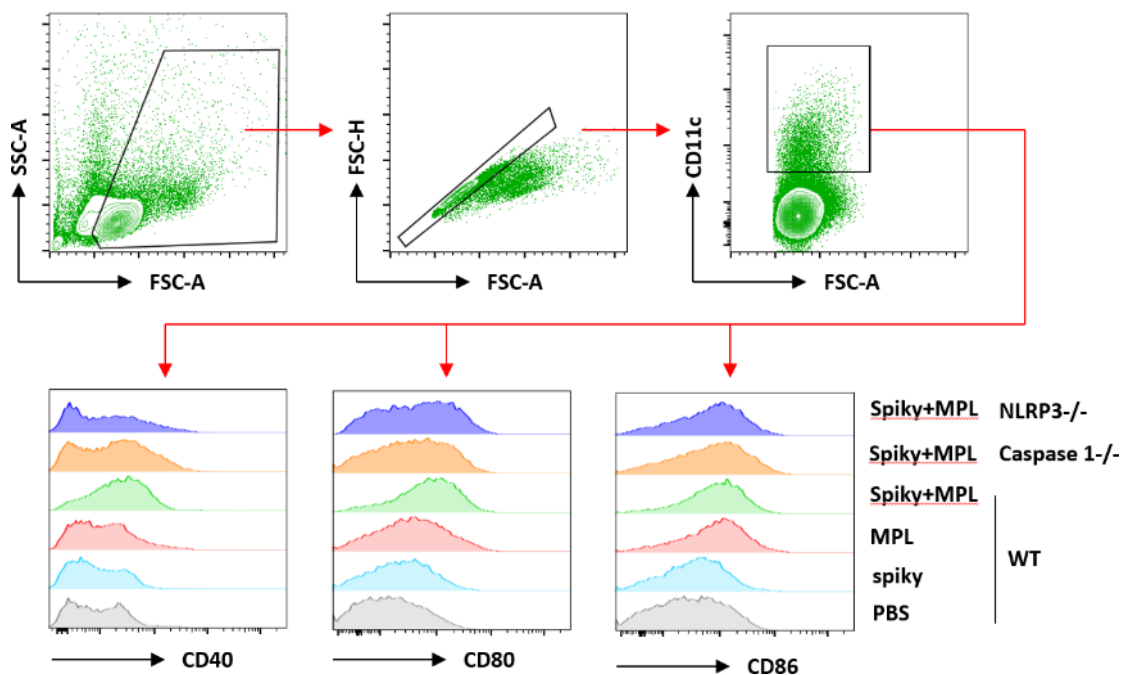


Figure S15. Analysis of DCs in draining lymph nodes. Wild-type, NLRP3^{-/-} or Caspase 1^{-/-} mice received subcutaneous injections of OVA with or without spiky particles, MPL or Spiky+MPL. The draining lymph nodes were collected 36 hours later for flow cytometry. Single cells were gated on FSC-H and FSC-A and expressions of CD40, CD80 and CD86 were analyzed on gate of CD11c⁺ DCs.

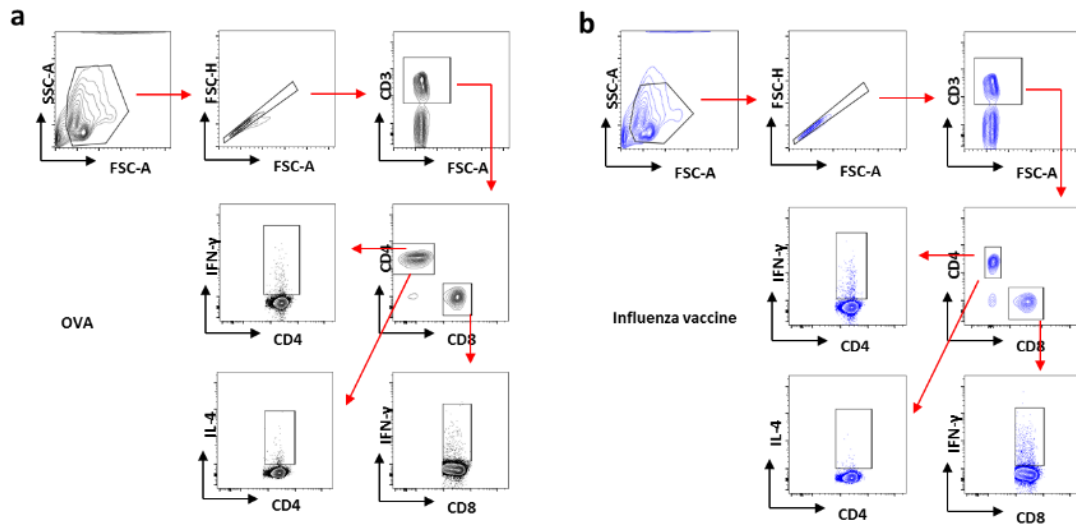


Figure S16. Gating strategies for T cell responses. Single cells were firstly gated in the basis of FSC-H and FSC-A. CD4⁺ and CD8⁺ T cells were analyzed for IL-4 and IFN- γ expression on the gate of CD3⁺ T cells. (a) The gating strategy for Figure 6e, f. Cellular immune responses induced by OVA. (b) The gating strategy for Figure 6i-j. Cellular immune responses induced by Influenza vaccine.

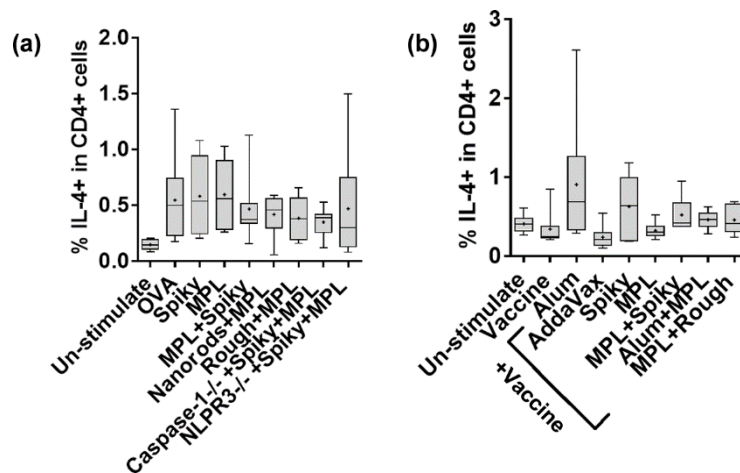


Figure S17. Spiky particles and MPL had no effect on antigen-specific IL-4⁺CD4⁺ T cells. (a) Wild-type or Caspase 1^{-/-} mice received s.c. injection of OVA alone or along with spiky particles, rough particles, nanorods, MPL or their combinations. CD4⁺ T cells secreting IL-4 were quantified 7 days later. From left to right, n=6, 14, 8, 8, 20, 12, 12, 12, 6 mice. (b) Mice were immunized on day 0 and day 14 with 2009 H1N1 monovalent influenza vaccine with indicated adjuvants, including AddaVax (50

$\mu\text{l}/\text{mouse}$), Alum (1 mg/mouse), spiky (1 mg/mouse), MPL (10 $\mu\text{g}/\text{mouse}$) or Spiky+MPL. CD4+ T cells secreting IL-4 were measured 5 days after the final immunization. n=6 mice, except for vaccine and AddaVax in which n=8. Data are presented as box and whiskers, in which whiskers are min-to-max. Mean is shown as “+”. All experiments were repeated twice with similar results.

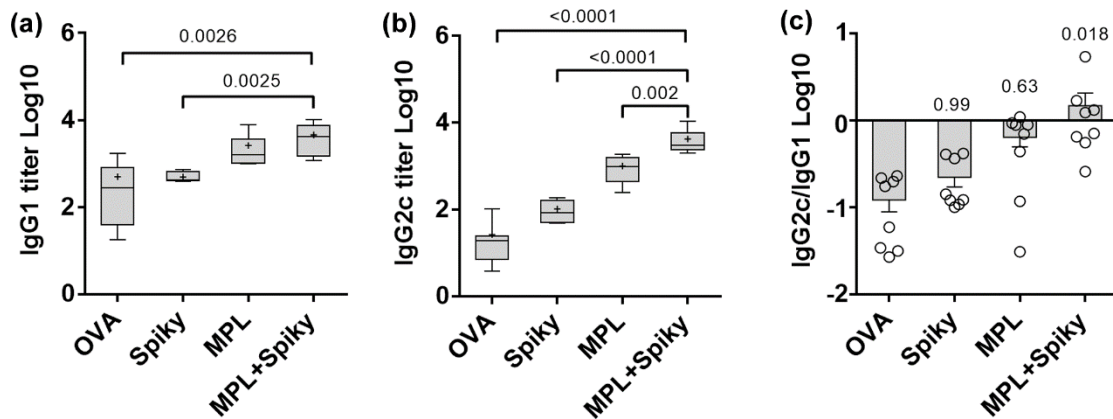


Figure S18. Combination of Spiky particles and MPL induced Th1-biased immune responses. C57BL/6 mice received subcutaneous injection of OVA with or without spiky particles, MPL or Spiky+MPL. (a) and (b) Serum IgG1 and IgG2c antibody titers were determined 14 days after immunization. n=8 mice. Data are presented as box and whiskers, in which whiskers are min-to-max. Mean is show as “+”. Significance between indicated groups was calculated by one-way ANOVA. (c) The ratio of IgG2c/IgG1. n=8 mice. All groups were compared to OVA alone by one-way ANOVA. All experiments were repeated twice with similar results. Data were presented as Mean \pm SEM.

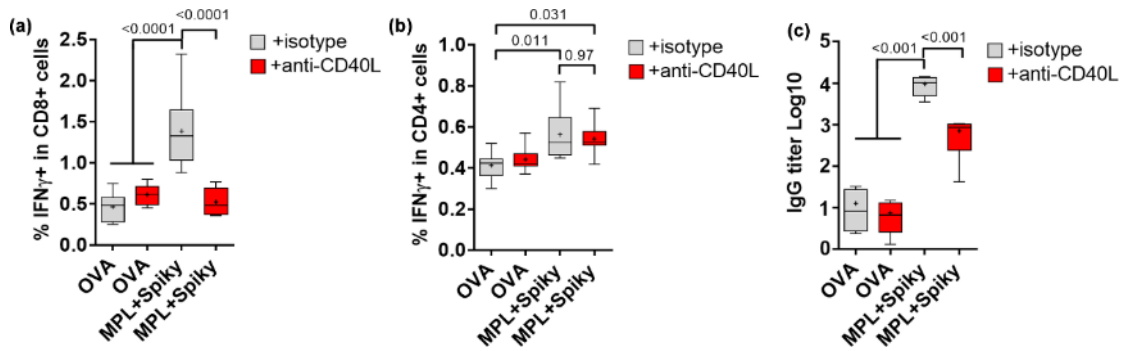


Figure S19. The adjuvant effect of MPL+Spiky depended on CD40-CD40L pathway. Mice received subcutaneous injections of OVA with or without Spiky+MPL. Some mice received anti-CD40L antibodies or isotype controls on day 0 and day 2 after immunization. (a, b) Cellular immune responses including IFN- γ secreting CD8 (a) and CD4 (b) T cells were measured 7 days after immunization. from left to right, n=8, 7, 8, 8 mice. (c) Serum IgG antibody titers were determined 12 days after immunization. n=4 mice. All experiments were repeated twice with similar results. Data of immune responses were presented as box and whiskers, in which whiskers are min-to-max. Mean is show as “+”. Significance between indicated groups was calculated by one-way ANOVA.

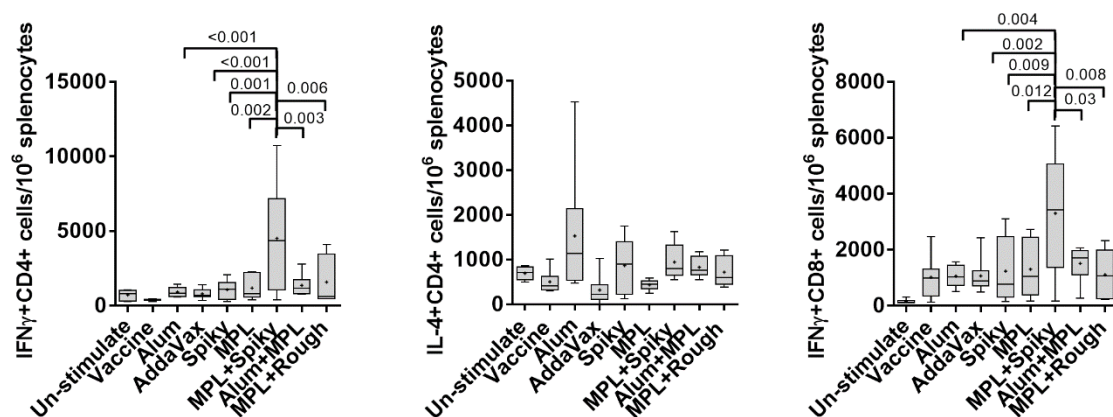


Figure S20. Numbers of cytokine-producing cells for Fig. 6i-j and Fig. S8.4b. n=6 mice, except for vaccine and AddaVax in which n=8. All experiments were repeated twice with similar results. Data of immune responses were presented as box and

whiskers, in which whiskers are min-to-max. Mean is show as “+”. Significance between indicated groups was calculated by one-way ANOVA.

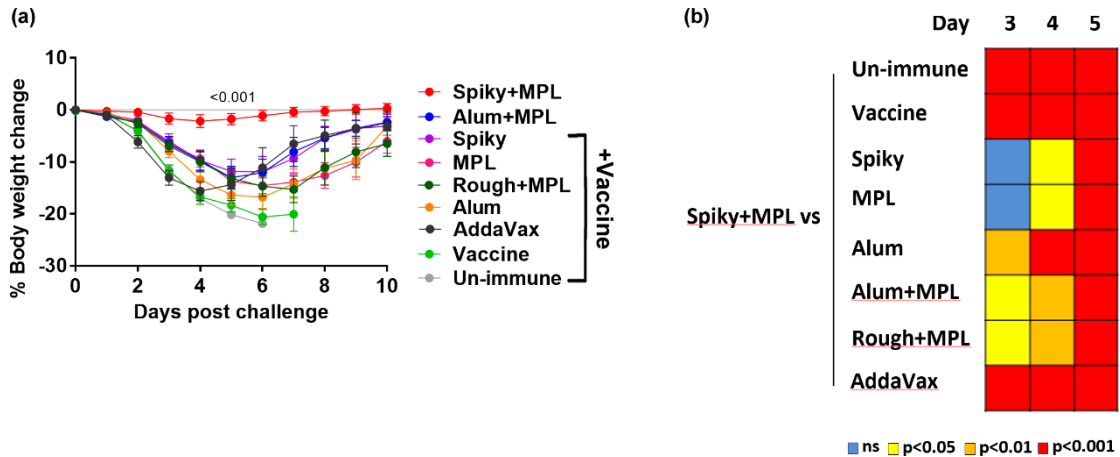


Figure S21. Body weight change after influenza viral challenge. (a) The immunized mice were challenged with 20×LD50 A/California/7/2009 H1N1 influenza virus 14 days after the final immunization. Body weight loss was monitored for additional 12 days. n=10 mice, except for vaccine and AddaVax in which n=12. (b) Body weight changes of the Spiky+MPL group were compared with other groups by one-way ANOVA. Data were summarized as a heat map. All experiments were repeated twice with similar results.

Supplementary References:

[1] VanDuin D, Cleare W, Zaragoza O, Casadevall A, Nosanchuk JD. (2004) Effects of Voriconazole on *Cryptococcus neoformans*. *Antimicrob Agents Chemother*, **2004**, 48(6): 2014-20.

[2] Waskman G, and Hultgren JS. Structural Biology of the Chaperone–usher Pathway of Pilus Biogenesis. *Nature Reviews Microbiology*, **2009**, 7, 765-774

[3] Medzhitov, R. Toll-like receptors and innate immunity. *Nature Reviews Immunology* 1, 135-145 (2001).

[4] Brubaker, S.W., Bonham, K.S., Zanoni, I. & Kagan, J.C. Innate Immune Pattern Recognition: A Cell Biological Perspective. *Annual Review of Immunology* 33,

257-290 (2015).

[5] Martinon, F., Burns, K. & Tschopp, J. The inflammasome: A molecular platform triggering activation of inflammatory caspases and processing of proIL-beta. *Molecular Cell* 10, 417-426 (2002).

[6] Broz, P. & Dixit, V.M. Inflammasomes: mechanism of assembly, regulation and signalling. *Nature Reviews Immunology* 16, 407-420 (2016).